Surface modification of 316L stainless steel with plasma nitriding

A. F. Yetim[1], F. Yildiz[2], A. Alsaran[1], A. Çelik[1]*

[1] *Department of Mechanical Engineering, Ataturk University, 25240 Erzurum, Turkey*
[2] *Aşkale College of Vocational, Ataturk University, 25240 Erzurum, Turkey*

Received 24 July 2007, received in revised form 5 November 2007, accepted 31 January 2008

Abstract

Plasma nitriding treatment of 316L austenitic stainless steel has been performed in 80%H_2-20%N_2 gas mixture, for various treatment times (1, 4 and 8 h) and at relatively low temperatures (400, 450 and 500 °C). Mechanical and tribological properties of the plasma nitrided 316L stainless steel were examined using X-ray diffraction, microhardness tester, scanning electron microscopy and pin-on-disc tribotester. The results show that the modified surface specimens of nitrided 316L stainless steel at 400 °C consist mainly of s-phase and small chromium nitride precipitates. At higher temperatures both CrN and iron (γ'-Fe_4N) nitrides have been observed and their amount increases with increasing treatment temperature. The highest hardness values were attained at 500 °C and 8 h, an increase of surface hardness was observed with increasing process time. Also wear resistance was improved after nitriding. The wear rate decreased with increasing process time and temperature. After electrochemical measurement it is observed that the corrosion resistance of nitrided 316L steel is getting worse in the modified layer unless the layer consists completely of s-phase and has an adequate continuous layer which covers whole surface of the specimen.

K e y w o r d s: plasma nitriding, 316L stainless steel, s-phase, wear, electrochemical measurements

1. Introduction

Austenitic stainless steels have a widespread use in many industrial applications among which are the food and chemical processing, automotive industry, some surgical implants, etc., because they exhibit a very high corrosion resistance in many aggressive environments due to passive Cr_2O_3 surface film. Although they have excellent corrosion resistance, surface hardness, friction coefficient and wear resistance of these materials are relatively poor. The improvement of the hardness and the tribological properties of austenitic stainless steel, especially well known 316L stainless steel, is a significant problem of high technological interest. Nowadays, there are many surface modification methods which improve these properties spanning from conventional plasma nitriding to plasma source ion implantation and reactive magnetron sputtering [1–3]. However, in most cases, an increase in the surface hardness results in a decrease in corrosion resistance compared to untreated stainless steel. This effect is due to CrN or Cr_2N formation in the modified diffusion layer.

The plasma nitriding is one of the well-known processes for surface modification of steels. Plasma nitriding is utilized to improve the fatigue strength, wear and corrosion resistance of both traditional and new materials [4–7]. In the studies on nitriding at low temperatures, it has been stated that the modified layer consists essentially of a metastable phase, which has proved to have high hardness and very good corrosion resistance. But, its structure is still a matter of debate and not completely clarified. Firstly, this phase has been described by Ichii et al. [8] as s-phase and later reported by other authors. It is also referred to as supersaturated austenite [9] or nitrogen-expanded austenite 'γ_N' [10]. Angelini et al. [11] first identified the structure of this phase as body-centered tetragonal (bct) and considered it as ε'. Marchev et al. [12, 13] confirmed the btc structure for this phase and named it as s-phase. Borgioli et al. [14] reported that the s-phase has a face centered cubic (fcc) structure with

*Corresponding author: tel.: +90442 231 4502; fax: +90442 236 0957; e-mail address: ayhcelik@atauni.edu.tr

high density of stacking faults. Fewell et al. [15] pointed out that triclinic unit cell is the best description of this phase.

It has been established by some studies that the process temperature and time are the most effective parameters in the development of surface structure. Fossati et al. [16] observed that modified layer thickness and the surface hardness increase with increasing treatment time. In another study it has been seen that the surface hardness increases with increasing treatment temperature. Although above 450 ℃ hard CrN and Fe_4N precipitates occur, the corrosion resistance of the stainless steel decreases. So the stainless steels are relatively treated at low temperature (up to 450 ℃) comparing to low alloy steels or tool steels to avoid CrN formation and to increase wear resistance without occurring an adverse effect on corrosion resistance [10]. Some researchers investigated the effect of plasma nitriding on corrosion resistance of stainless steels in different environments. They reported that plasma nitriding above 500 ℃ decreased the corrosion resistance of stainless steels because of CrN formation, in spite of increasing both hardness and modified diffusion layer thickness [17–19]. In addition, Menthe et al. [1] observed that the wear rate after plasma nitriding was reduced considerably compared to the untreated samples.

Although there are a lot of studies related to the behaviour of nitrided 316L stainless steel, the effect of layers formed on the surface and usage of the nitrided 316L stainless steel as implant material are still a debate issue. In this context, the objective of present work is to study the effects of treatment time and temperature on microstructure, morphology, microhardness, wear, and corrosion properties of plasma nitrided 316L austenitic stainless steel. The variations of structural, mechanical, tribological, and corrosion properties of AISI 316L steel after plasma nitriding treatment were investigated using X-ray diffraction (XRD), scanning electron microscopy (SEM), microhardness tester, pin-on-disc tribotester, electrochemical polarization and impedance spectroscopy.

2. Experimental details

AISI 316L stainless steel, whose chemical composition is given in Table 1, has been used in the experiments. The specimens were cut from cylindrical bars with diameter of 18 mm and thickness of 9 mm. The samples were grinded by 220–1200 mesh emery papers, and then polished with alumina powder with 1 μm grain size. After cleaning with alcohol, the specimens were placed into the plasma nitriding chamber and the chamber was evacuated to 2.5 Pa. Prior to the process, to remove surface contaminates, the specimens were subjected to cleaning by hydrogen sputtering for 15 min under a voltage of 500 V and a pressure of 5×10^2 Pa. The plasma nitriding was performed in gas mixture of 80%H_2-20%N_2, process temperatures of 400, 450, 500 ℃ and process times of 1, 4, 8 h.

Table 1. Chemical composition of AISI 316L stainless steel (%)

C	Si	Cr	Mn	Mo	P	S	Ni
0.016	0.490	16.640	1.820	2	0.030	0.026	10.100

After the nitriding process, the modified layer formed on the surface was removed by polishing to observe metallographic examinations and to measure microhardness of the layer on the cross-section. Surface hardness and modified layer thickness were measured by using a Buehler Omnimet MHT1600-4980T instrument at a constant load of 10 g and loading time of 15 s. X-ray diffractometer Rigaku operated at 30 kV and 30 mA with Cu Kα radiation was used for XRD analysis. JCPDS cards were used for the phase's identification. The modified diffusion layer thickness was also investigated using a scanning electron microscope (SEM) Jeol 6400.

The wear tests were carried out on Teer POD-2 pin-on-disc tester, using a 5 mm diameter WC-Co ball as the pin. The friction force was monitored continuously by means of a force transducer. Unlubricated wear tests with a sliding distance of 141 m were carried out at room temperature (≈ 18 ℃), relative humidity of about 50 %, sliding speed of 0.078 m s^{-1}, normal load of 10 N and a wear track diameter of 10 mm. To calculate the wear volume, the profiles were recorded before and after the wear tests by a profilometer Mitutuyo. Then, from the superimposed profiles, the wear volume was calculated. The worn regions after the wear tests were examined using SEM.

Electrochemical polarization experiments were performed using a potentiostat, Potentioscan Wenking POS73. The electrodes were prepared by connecting a wire to one side of the sample that was covered with cold setting resin. One side of the specimen with an area of approximately 0.25 cm^2 was exposed to the solution. The polarization measurements were carried out in a corrosion cell containing ringer solution of 500 ml at 37 ℃. The electrochemical cell consisted of the specimens as the working electrode, a saturated calomel reference electrode and a platinum counter electrode. The specimens were immersed in the test solution, and a polarization scan was carried out towards more noble values at a rate of 1 mV s^{-1}, after allowing a steady state potential to develop. Also impedance measurements were carried out using Gamry PCI14/750 in ringer solution at 37 ℃. Impedance measurements were made in the frequency range from 20 kHz to 0.01 Hz with 10 mV amplitude. In all the experiments the open circuit potential was main-

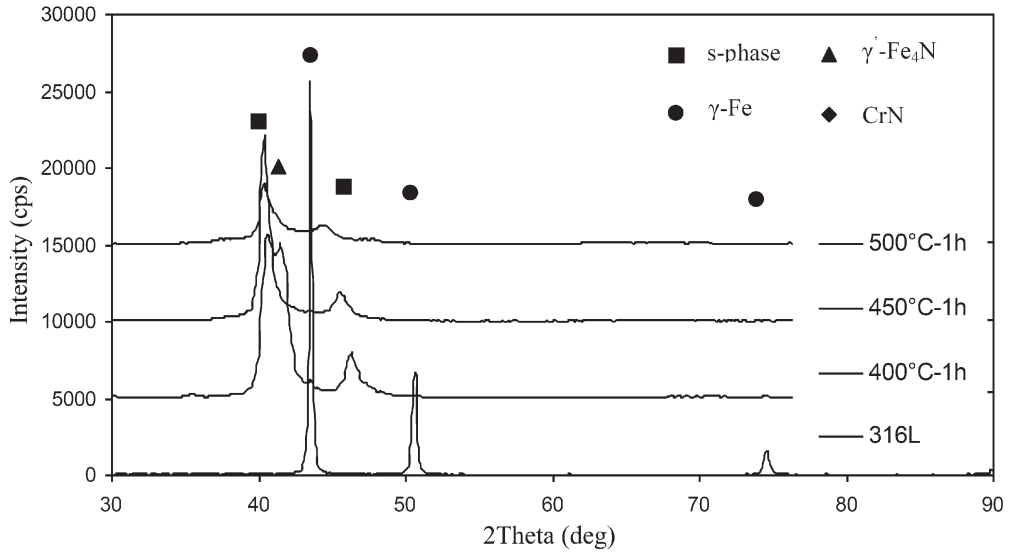

Fig. 1. XRD results of plasma nitrided 316L stainless steel at 400, 450 and 500 °C for 1 h.

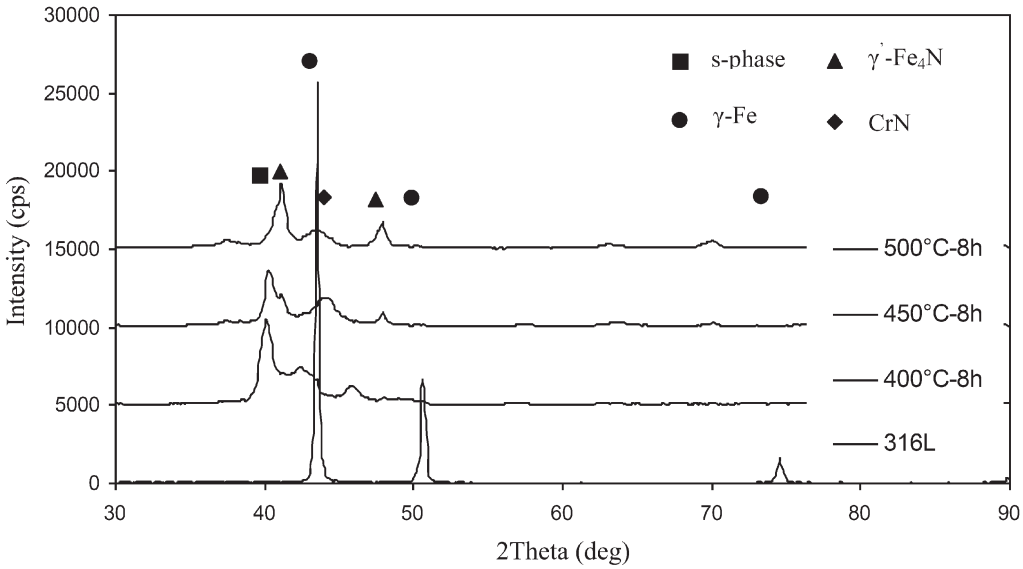

Fig. 2. XRD results of plasma nitrided 316L stainless steel at 400, 450 and 500 °C for 8 h.

tained for 2 h. NH_3 amounts were measured by WTE NOVA 60 spectrophotometers.

3. Results and discussion

3.1. XRD analysis

The variation of the XRD patterns with different treatment parameters is shown in Figs. 1–3. In the untreated 316L samples, the structure consists of austenite phase. In the case of the nitrided samples, XRD analysis shows that the nitriding process produced a modified layer on the substrate. The main phase in the modified layer is s-phase or expanded austenite (γ_N) which has proved to have high hardness and very good corrosion resistance.

Figure 1 shows the effect of treatment temperature on the 316L samples for 1 h process time. At 400, 450 and 500 °C, the modified layer mainly consists of metastable s-phase. In the fact, the formation of s-phase is concerned with diffusion of nitrogen from the plasma atmosphere and chromium atoms from the substrate. That is, at 400 °C, the diffusion of nitrogen as an interstitial element to the iron lattice is greatly encouraged whilst the diffusion of chromium as a substitution element is prohibited [21]. Thus, austenite lattice with the effect of nitrogen atoms expands and then, this structure is defined as expanded austenite. At the temperatures up to 450 °C and for short process times,

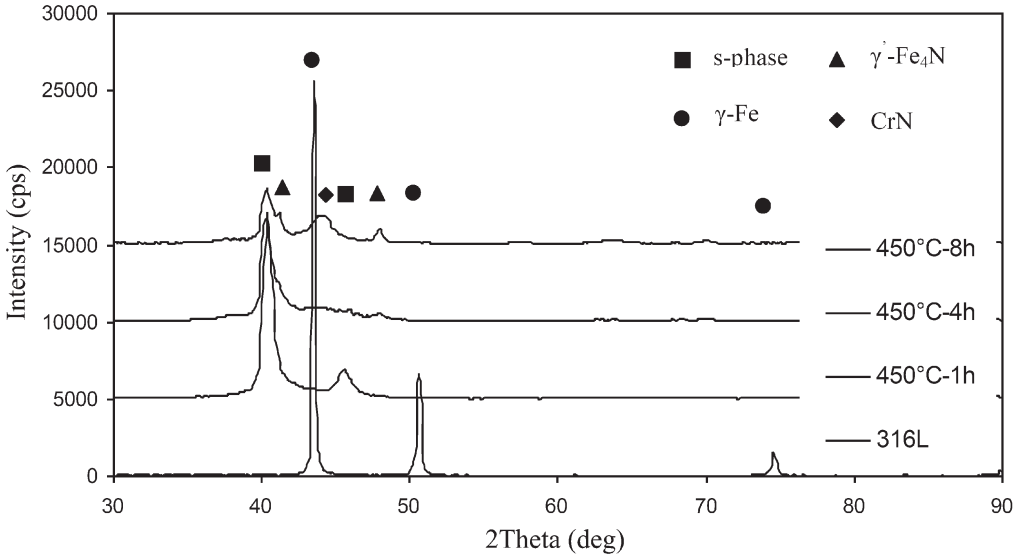

Fig. 3. XRD results of plasma nitrided 316L stainless steel at 450 °C for 1 h, 4 h and 8 h.

chromium nitride (CrN or Cr_2N) formation tendency is low. So, the chromium does not precipitate as nitride and remains in solid solution for the formation of a passive oxide film.

When Figs. 1 and 2 are evaluated, the formation of CrN and γ'-Fe_4N nitrides has been observed together with s-phase in the modified layer as the temperature increases. When the temperature of 450 °C is reached, the activation of Cr atoms increases, and CrN starts to form. Initially, nitrogen atoms leave the planes of the s-phase and if processing continues, CrN nucleates and grows at the presence of expanded austenite [22]. Therefore, CrN and Fe_4N are formed due to partial decomposition of the metastable expanded austenite phase. It may be assumed that nitrides become more stable as temperature increases and the metastable s-phase tends to transform into the γ'-Fe_4N nitride.

The formation of s-phase depends essentially on the process temperature and time is also an important parameter. XRD results obtained from experimental studies performed with the aim to define the effect of treatment time on nitriding of AISI 316L stainless steel are given in Fig. 3. It was seen that modified layers of specimens nitrided at treatment times of 1 h and 4 h consisted of mainly s-phase. By increasing the treatment time, the nitride formation tendency increases. Whilst the s-phase only forms after treatment of 1 h, when the time is increased to 4 h, γ'-Fe_4N peaks together with s-phase are detected. If the nitriding process is performed for 8 h, besides s-phase, the presence of CrN and γ'-Fe_4N nitrides is observed. With increasing treatment time, the intensity of s-phase peaks decreases and the intensity of CrN peaks increases. It has to be noted that a large amount of CrN precipitates has the main responsibility for the loss of corrosion resistance of austenitic stainless steel. It has been observed that the diffraction peak set shifts towards to the left (lower diffraction angles) as the nitriding time increases. The shifting of the peaks is clearly shown in Fig. 3. This may indicate that longer nitriding time causes lattice distortion because of larger amount of the nitrogen concentration in the modified layer. By increasing lattice distortion strength and increasing the hardness, the shift in the peak position of different planes is different due to the difference of the amount of lattice distortion. It may be supposed that nitrogen concentration is larger in the plane where the shift is larger than in the other planes [23].

3.2. Microstructure and morphology

The SEM micrographs of the plasma nitrided and untreated samples are given in Fig. 4. While untreated samples exhibit a typical austenitic morphology, treated samples show a special morphology (Fig. 4a). In the case of treated samples, the surface appears like plasma etched because of sputtering and treatments themselves (Fig. 4b). After treatments, it has been observed that the grains corresponding to the austenitic substrate have continuity on surface layer. Additionally, slip bands appear within the grains of the treated samples after chemical etching with %20HNO_3-%30HCL-%50Glycerin.

The surface of all the nitrided samples appears to be a homogeneous layer separated from the bulk material by a clear line. The mean thickness of this layer is given in Table 2. The thickness of modified layer was measured between 5–80 μm. The minimum thickness has been obtained from the samples nitrided at 400 °C and for 1 h. It has been observed that the thickness of the modified layer increases as the treatment temperature and time increase. Also, the sur-

Table 2. Changes in modified layer thickness, surface roughness and surface hardness of nitrided AISI 316L for different parameters

Number	Nitriding parameters			Modified layer thickness (μm)	Surface roughness (R_a)	Hardness $HK_{0.01}$	d-spacing ($2\theta = 43.5^\circ$)
	Temperature (℃)	Time (h)	Gas mixture				
1	400	1		3–5	0.05–0.08	600–630	0.22255
2	400	4		9–12	0.08–0.11	890–920	0.22522
3	400	8		12–14	0.14–0.17	1175–1200	0.22522
4	450	1		6–9	0.14–0.19	1050–1080	0.22414
5	450	4	$20\%N_2 + 80\%H_2$	17–20	0.30–0.43	1150–1200	0.22361
6	450	8		30–35	0.33–0.46	1420–1450	0.22414
7	500	1		12–15	0.21–0.39	970–1000	0.22255
8	500	4		40–45	0.24–0.27	1300–1350	0.2204
9	500	8		77–80	0.37–0.43	1650–1700	–
Untreated 316L				–	0.05–0.08	270–300	0.20742

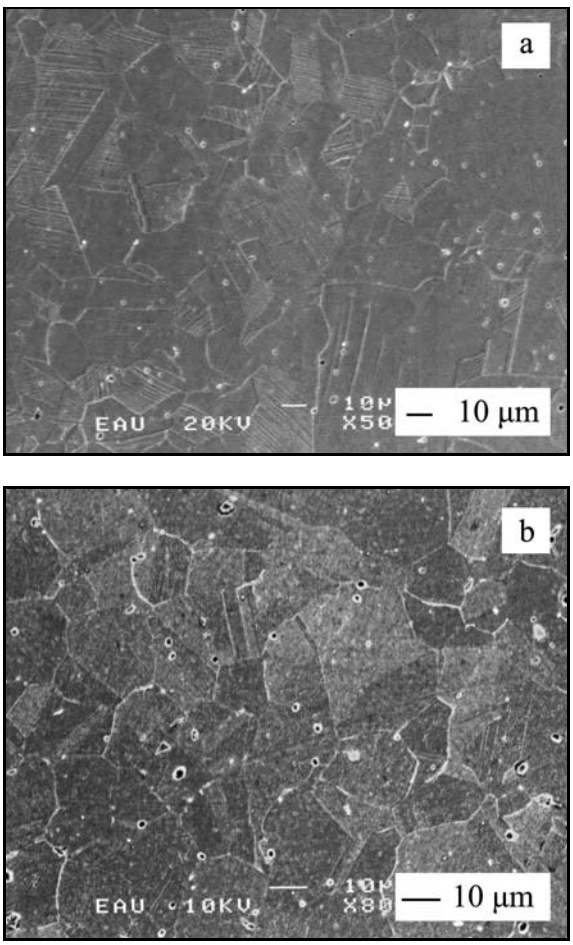

Fig. 4. Surface morphology of 316L stainless steel: (a) untreated, (b) nitrided at 500 ℃ for 8 h.

face roughness increases with increasing process time (Table 2).

The surface layers show different characteristics dependent on the process temperature and time. The main phase to be formed at 400 ℃ is expanded austenite (s-phase) and this phase appears as a white area in the modified layer. By increasing temperature and time, CrN and γ'-Fe_4N nitrides start forming and they appear as dark spots [24]. When the treatment temperature reaches 500 ℃, the amount of the nitrides (dark areas) increases and covers the whole layer (Fig. 5a). At 500 ℃, s-phase (white areas) decreases in the modified layer. In addition, it has been noted that a lot of microcracks have formed through the nitride layer as treatment temperature increases. It can be concluded that the microcracks are formed due to differences in internal stresses between the CrN and γ'-Fe_4N decomposition products of the s-phase (Fig. 5b).

3.3. Microhardness

The change of microhardness values of the surface layers with treatment temperature and time is given in Table 2. The plasma nitrided samples show higher surface hardness than the untreated ones. The microhardness of untreated samples was measured as 270–300 $HK_{0.01}$. All the treated samples show high hardness values in the modified layer, and then the hardness decreases to that of the substrate values under the line that separates the modified layer from the substrate. After the treatment, the minimum hardness 600–630 $HK_{0.01}$ (at 400 ℃ for 1 h) and the maximum hardness 1650–1700 $HK_{0.01}$ (at 500 ℃ for 8 h) have been measured. The microhardness of the surface increased 2–6 times depending on process parameters. The microhardness value of the plasma nitrided surface depends on the thickness of the modified layer. As the treatment time increases, the thickness of layer increases in agreement with the morphological observations.

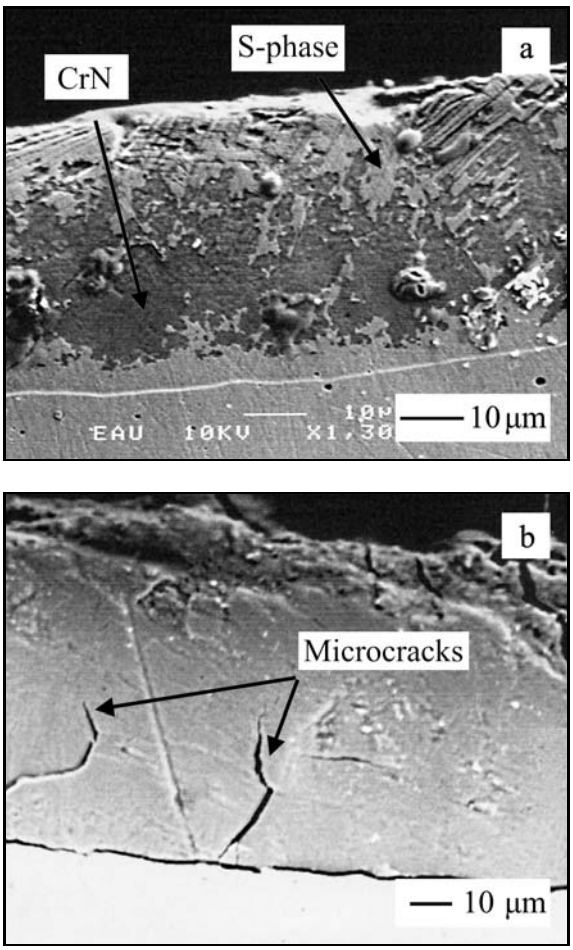

Fig. 5. SEM micrograph of the modified layer: (a) s-phase and CrN precipitates in sample nitrided at 500 °C for 4 h, (b) microcracks in the modified layer of sample nitrided at 500 °C for 8 h.

The samples treated at 500 °C show very high microhardness values compared to the samples treated at 400 °C and 450 °C. Even if the hardness of the s-phase is lower than that of the dual phase nitride (CrN + γ'-Fe_4N), s-phase has high hardness due to lattice distortion caused by interstitial nitrogen atoms. As a matter of fact, XRD analysis revealed higher distortion for the samples treated longer times.

3.4. Friction and wear

Friction test results of plasma nitrided AISI 316L stainless steel are illustrated in Fig. 6. The friction coefficients of the plasma nitrided samples are generally between 0.5–0.6. At the beginning of the friction test, the friction coefficient increases due to Hertizan contact, then, it becomes stable. It should be noted that the friction coefficient suddenly decreases to 0.35 after plasma nitriding at 450 °C for 1 h.

The lowest wear rate has been obtained from nitrided samples at 500 °C for 8 h (Fig. 7), because the intense phases in this process condition are than CrN and γ'-Fe_4N dual phase structure which has high hardness. The wear rate decreases as the amount of CrN and γ'-Fe_4N increase although CrN and γ'-Fe_4N phases may bring breakability properties to the modified layer. During the wear of samples consisting mainly s-phase, relatively soft s-phase is plastered to the ball and then, soft-soft contact has been provided. Thus, wear rate decreases. However, the presence of excessively thin compound layer to measure causes the appearance of an abrasion wear component because the layer breaks down during the sliding and forms hard abrasive particles [7]. In the initial period of sliding, the brittle compound layer with high stress frac-

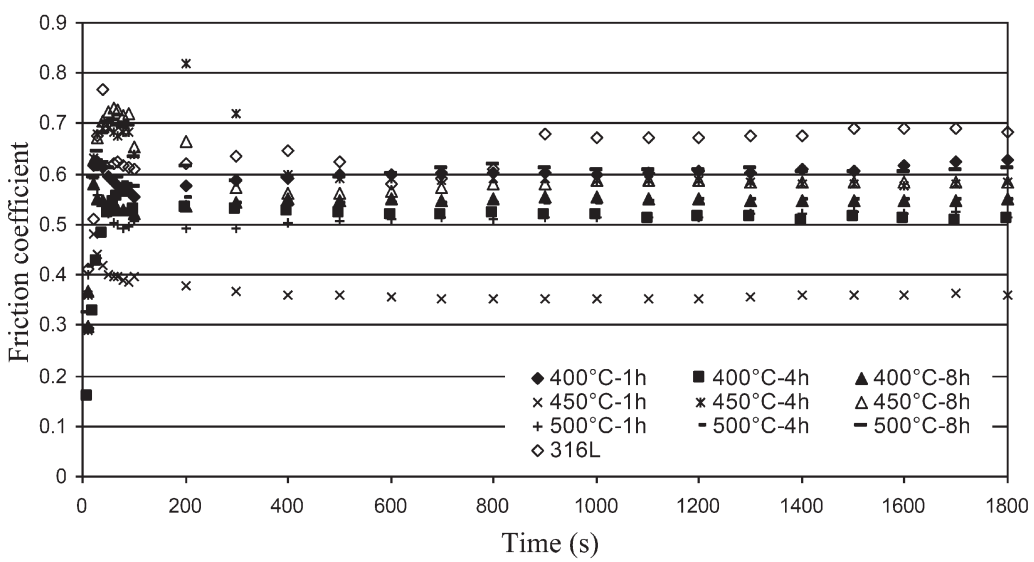

Fig. 6. Friction test results of nitrided 316L stainless steel.

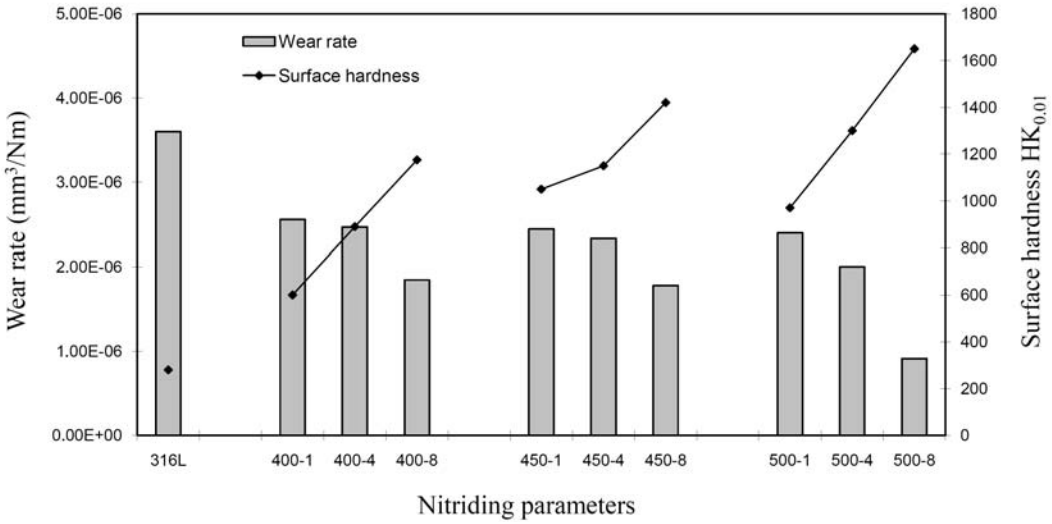

Fig. 7. Wear rate and surface hardness results of nitrided 316L stainless steel.

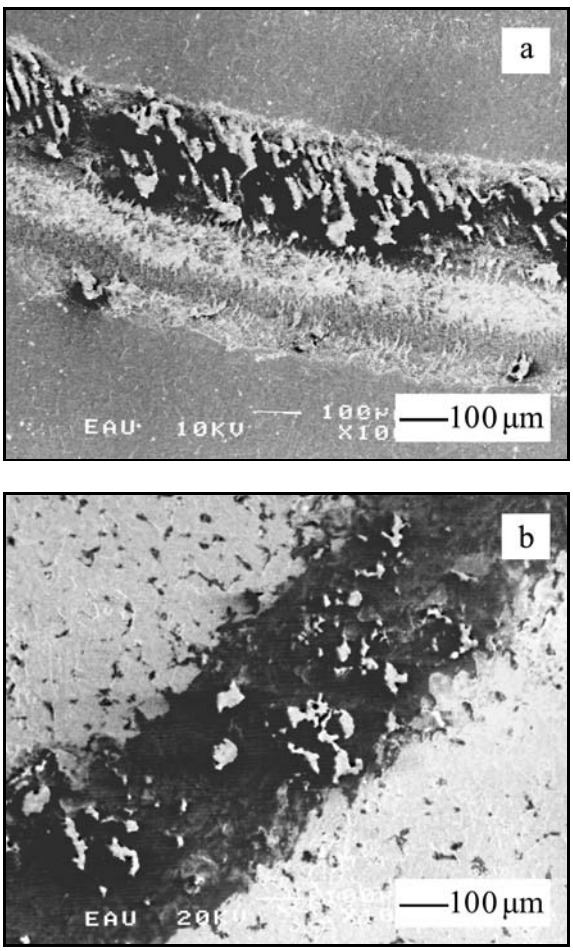

Fig. 8. SEM micrographs of wear tracks of the untreated (a) and the plasma nitrided for time of 1 h at temperature of 450 ℃ (b).

tured and then transformed abrasive particles. The profiles of the plasma nitrided samples are smoother and more stable. In addition, less failure was observed compared to untreated specimen. Initially, a wear begins as plugging, and then the debris separate from track and embed in wear track during motion. So it can be said that the particles facilitate abrasive wear. The wear profiles of the plasma nitrided and untreated AISI 316L are given in Fig. 8. When comparing Figs. 8a,b, the wear track of the untreated sample is larger than that of nitrided sample and the particles are not observed along the wear track. It can be seen that the prevailing mechanism is adhesive wear, which is found for all the nitrided samples.

3.5. Electrochemical studies

Open circuit measurements were carried out for the untreated and nitrided specimens in ringer solution containing 0.086 g NaCl, 0.033 g $CaCl_3$ and 0.03 g KCl per 100 ml. The experimental results are given to prevent overlap in Fig. 9. The potential was measured for 60 min prior to polarization experiments as shown in Fig. 10. Open circuit potential (OCP) was found to move away from noble direction for all the nitrided specimens when compared to 316L. As can be seen in Fig. 9, the potential shifted in the negative direction for all the nitrided specimens, which clearly indicates breaks in the film, dissolution of the film, or no protective film formation.

Figures 10–12 depict polarization curves for the untreated and the nitrided 316L steel. As is seen in Table 3 and Figs. 10–12, the corrosion current density values (I_{corr}) of nitrided 316L steel at temperature of 400 ℃ were lower than those of other nitrided and untreated specimens. It was found that the minimum current density and voltage are for 400 ℃ and 1 h for the nitrided and the untreated specimens, respectively. The corrosion behaviours of the nitrided

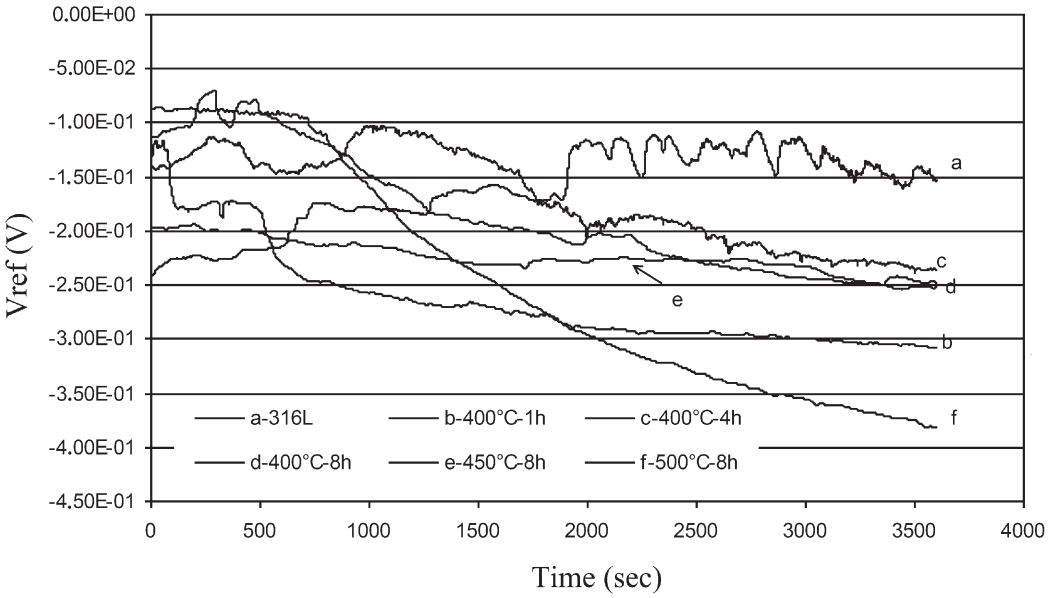

Fig. 9. Change of OCP potential and time for untreated and nitrided 316L stainless steel.

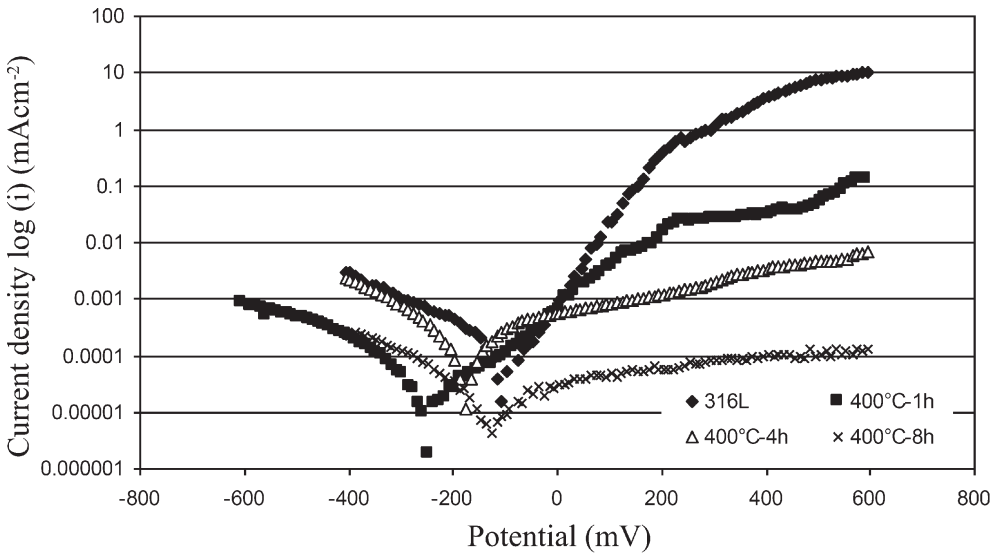

Fig. 10. Polarization curves for plasma nitrided 316L stainless steel at 400 °C for 1 h, 4 h and 8 h.

specimens are related to the thickness of the modified layer, and phase type occurs during nitriding. If the modified layer includes s-phase and has adequate thickness, the corrosion resistance increases compared to untreated 316L. An adequate thickness for modified layer means a continuous layer which covers whole surface of the specimen and is not to be affected by surface discontinuities. The corrosion resistance properties of s-phase can be ascribed to its very high nitrogen content. It is known that a little amount of interstitial nitrogen in austenitic stainless steels allows to increase their pitting corrosion resistance sensibly [24]. When an austenitic stainless steel containing interstitial nitrogen is subjected to pitting corrosion interstitial nitrogen atoms are released. The released nitrogen atoms can react with H^+ to form NH_3 [25]. Owing to this cathodic reaction the local pH increase allows to facilitate the repassivation. As seen in Table 3, both the amounts of pH and NH_3 of the specimens nitrided at 500 °C are high and polarization curves show a passive region. However, the thickness of modified layer obtained is relatively large and the CrN precipitates are present in large amount (Figs. 2 and 3), when the nitriding time and temperature increase. Next to CrN precipitates, the Cr-depleted zones do not contain a sufficiently high chromium concentration, and they are subject to active corrosion process.

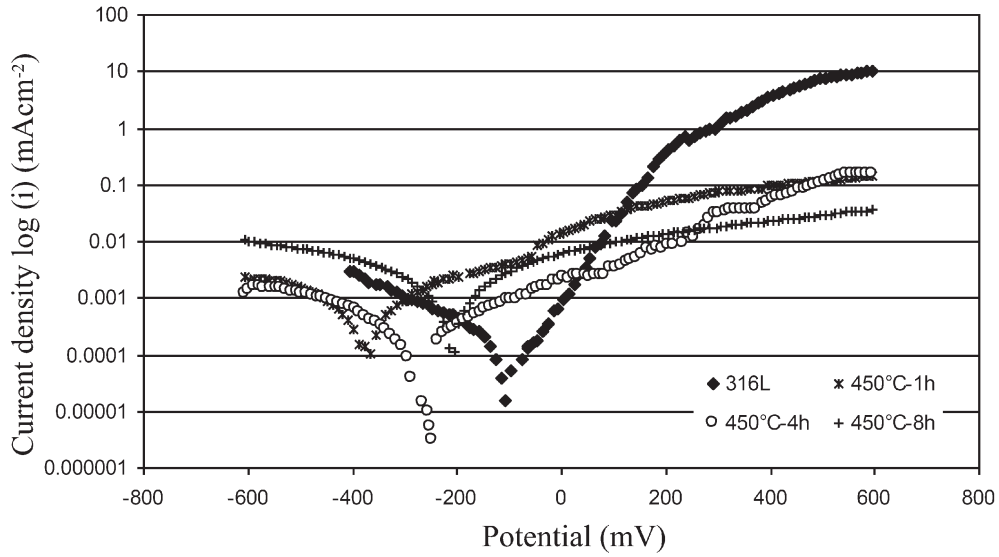

Fig. 11. Polarization curves for plasma nitrided 316L stainless steel at 450 ℃ for 1 h, 4 h and 8 h.

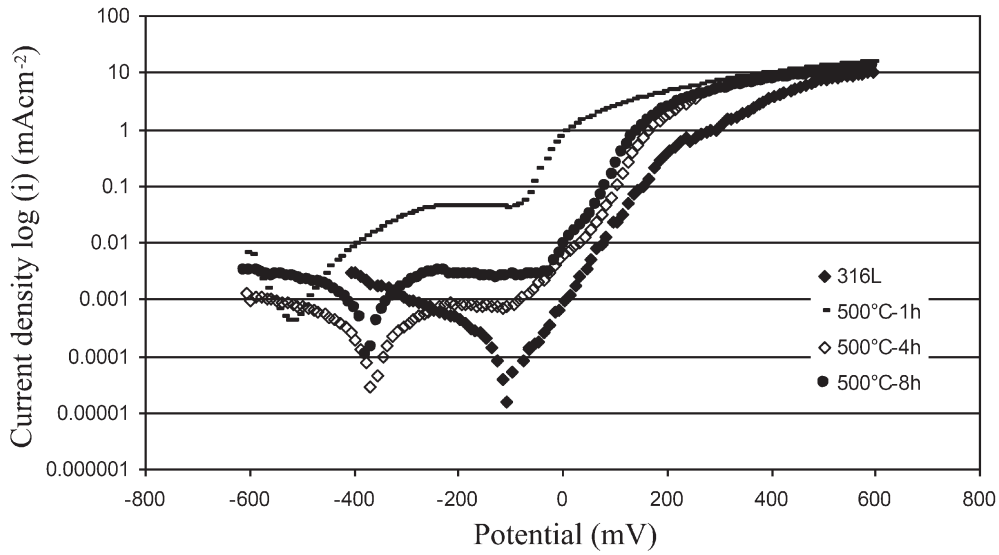

Fig. 12. Polarization curves for plasma nitrided 316L stainless steel at 500 ℃ for 1 h, 4 h and 8 h.

Table 3. The polarization results of nitrided AISI 316L for different parameters

Number	Nitriding parameters			E_{corr} (mV)	I_{corr} (mA cm^{-2})	pH	NH_3 (mg l^{-1})
	Temperature (℃)	Time (h)	Gas mixture				
1	400	1		−233	3.47×10^{-5}	5.80	0.146
2	400	4		−179	1.82×10^{-4}	5.92	0.132
3	400	8		−140	1.74×10^{-5}	5.61	0.087
4	450	1		−384	1.07×10^{-3}	5.75	0.095
5	450	4	20%N_2 + 80%H_2	−266	1.78×10^{-4}	5.82	0.078
6	450	8		−204	1.90×10^{-3}	5.80	0.107
7	500	1		−542	1.20×10^{-3}	5.90	0.105
8	500	4		−345	2.24×10^{-4}	6.20	0.092
9	500	8		−340	1.01×10^{-4}	6.78	0.108
Untreated 316L				−83	1.50×10^{-4}	5.50	0.065

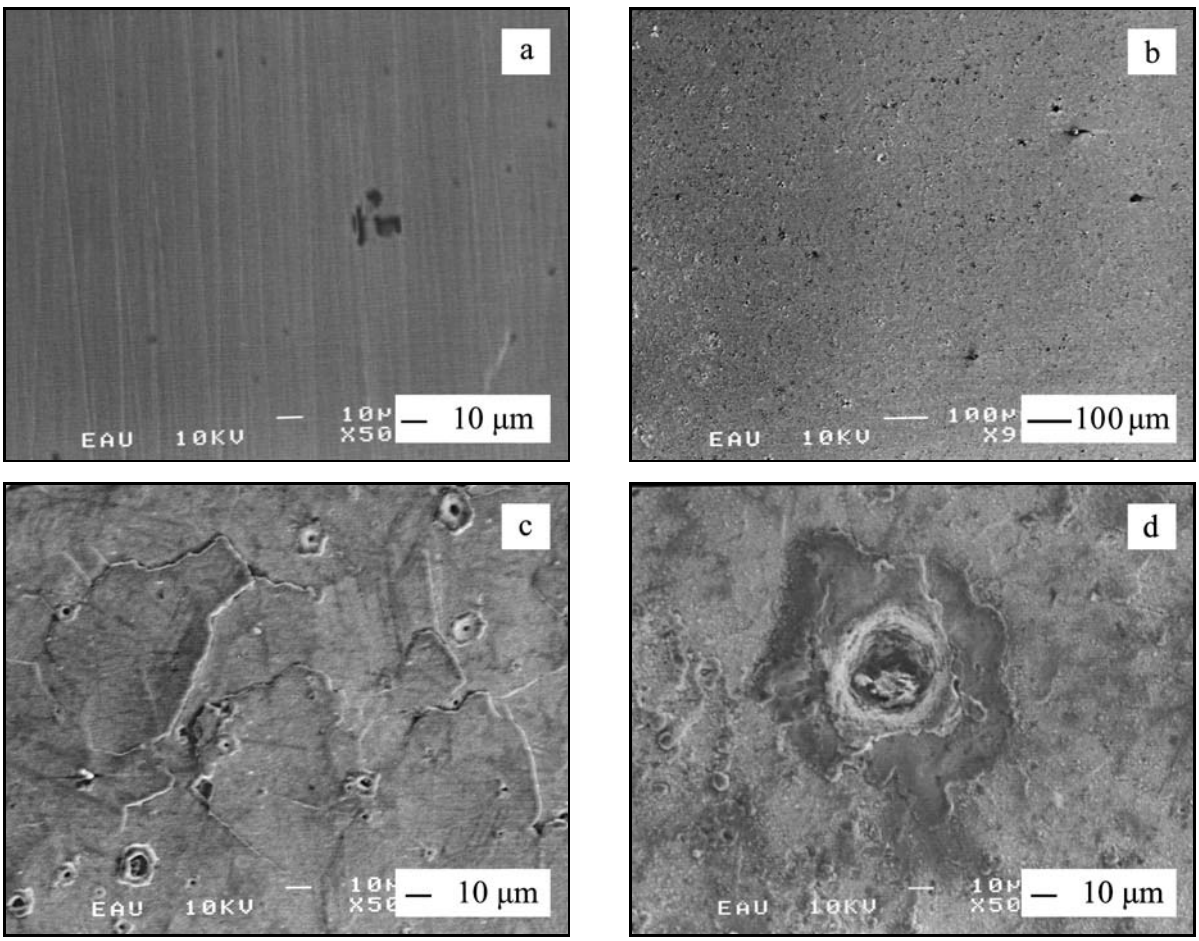

Fig. 13. SEM micrographs of corroded 316L samples: (a) untreated, (b) nitrided at 400 °C for 1 h, (c) nitrided at 450 °C for 4 h, and (d) nitrided at 500 °C for 8 h.

It was observed that abundant pitting corrosion occurs for the nitrided 316L stainless steel samples. This result is consistent with the suggestion that CrN is precipitated in the matrix of expanded austenite. Inhomogeneous microstructures enhanced corrosion due to electrolytic cell reaction between the second phase particles and the matrix. Therefore, when CrN precipitates result in substantial chromium segregation in 316L stainless steel, local galvanic cells will be set up which further enhance the pitting corrosion. The surface images of nitrided and untreated 316L steel after the corrosion tests are given in Fig. 13. When the SEM images were examined, the surface of specimens untreated and nitrided at low temperature (400 °C) appeared to be untouched (Figs. 13a,b). As seen in XRD graphs, in the modified layer mainly s-phase occurs up to nitriding temperature of 450 °C, and CrN starts occurring with increasing temperature. At 500 °C, the structure is mainly CrN. Therefore the nitrided specimens at higher temperatures exhibit the presence of many pits distributed on the surface as a result of the corrosion intensifying at a very narrow place (Figs. 13c,d).

The impedance behaviour of the specimens is expressed in Nyquist plots and given in Fig. 14. Although impedance dates overlap together, it is clearly seen that the impedance values of the nitrided 316L are lower than those of the untreated 316L. The untreated 316L steel has the highest corrosion resistance. Similar behaviour was obtained in the polarization measurements. The corrosion results show that the nitriding treatment did not bring the expected improvement in the corrosion resistance of the AISI 316L steel, and this system, in which especially CrN occurred, cannot be used for biomedical applications.

4. Conclusion

The structural and tribological properties of the plasma nitrided 316L stainless steel at different conditions have been investigated. While CrN and γ'-Fe_4N form after nitriding treatment at 500 °C, s-phase having low hardness and high wear resistance forms after nitriding at 400 °C and 450 °C. It has been observed that the diffraction peaks of s-phase shift towards

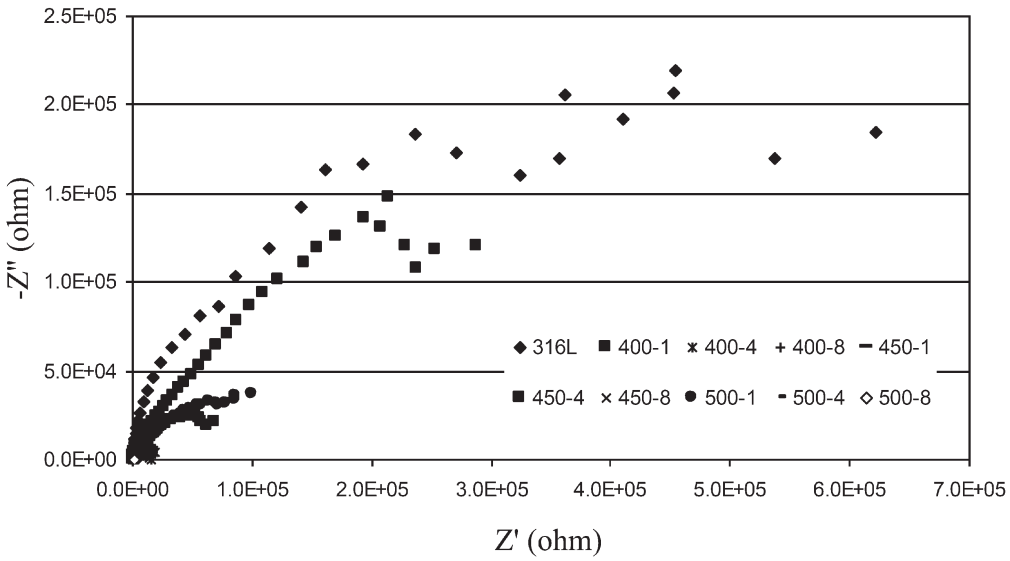

Fig. 14. Impedance diagrams for untreated and nitrided 316L.

the lower diffraction angles. The surface hardness increases with increasing both process temperature and time. Besides, s-phase has provided decreasing of the wear rate by preventing formation of abrasive particles because of its lower hardness than CrN and γ'-Fe_4N dual phases. It was observed that the corrosion behaviour of the nitrided specimens was related to the thickness of continuous modified layer and phase type which occurred during nitriding, and nitriding treatment did not bring the expected improvement in the corrosion resistance of the AISI 316L steel.

Acknowledgements

This research is part of the TUBITAK (The Scientific and Technical Research Council of Turkey) project supported by grant no. 104M222.

References

[1] LI, X. Y.: Surface Eng., *17*, 2001, p. 147.
[2] ZHU, X. M.—LEI, M. K.: Surf. Coat. Technol., *131*, 2000, p. 400.
[3] PICARD, S.—MEMET, J. B.—SABOT, R.: Mater. Sci. Eng. A., *303*, 2001, p. 163.
[4] EDENHOFER, B.: Metal Process, *109*, 1976, p. 38.
[5] CELIK, A.—ARSLAN, Y.—YETIM, A. F.—EFEOGLU, I.: Kovove Mater., *45*, 2007, p. 35.
[6] KARAMIS, M. B.: Wear, *147*, 1991, p. 385.
[7] ALSARAN, A.: Mater. Chart., *49*, 2002, p. 171.
[8] ICHII, K.—FUJIMURA, K.: Transactions of the Iron and Steel Institute of Japan, *27*, 1987, p. 263.
[9] HANNULA, S. P.—NENONEN, P.—HIRVONEN, J. P.: Thin Solid Films, *181*, 1989, p. 343.
[10] SAMANDI, M.—SHEDDEN, B. A.—SMITH, D. I.—COLLINS, G. A.—HUTCHINGS, R.—TENDYS, J.: Surf. Coat. Technol., *59*, 1993, p. 261.
[11] ANGELINI, E.—BURDESE, A.—DEBENETTI, B.: Metall. Sci. Technol., *6*, 1988, p. 33.
[12] MARCHEV, K.—COOPER, C. V.—BLUTCHER, J. T.—GIESSEN, B. C.: Surf. Coat. Technol., *99*, 1998, p. 225.
[13] MARCHEV, K.—HIDALGO, R.—LANDIS, M.—VALLERIO, R.—COOPER, C. V.—GIESSEN, B. C.: Surf. Coat. Technol., *112*, 1999, p. 67.
[14] BORGIOLI, F.—FOSSATI, A.—GALVANETTO, E.—BACCI, T.—PRADELLI, G.: Surf. Coat. Technol., *200*, 2006, p. 5505.
[15] FEWELL, M. P.—MITCHELL, D. R. G.—PRIEST, J. M.—SHORT, K. T.—COLLINS, G. A.: Surf. Coat. Technol., *131*, 2000, p. 300.
[16] BORGIOLI, F.—FOSSATI, A.—GALVANETTO, E.—BACCI, T.: Surf. Coat. Technol., *200*, 2005, p. 2474.
[17] FOSSATI, A.—BORGIOLI, F.—GALVANETTO, E.—BACCI, T.: Surf. Coat. Technol., *200*, 2006, p. 3511.
[18] PRIEST, J. M.—BALDWIN, M. J.—FEWELL, M. P.—HAYDON, S. C.—COLLINS, G. A.—SHORT, K. T.—TENDYS, J.: Thin Solid Films, *345*, 1999, p. 113.
[19] LIANG, W.—XIALOEI, X.—JIUJUN, X.—YAQIN, S.: Thin Solid Films, *391*, 2001, p. 11.
[20] JEONG, B. Y.—KIM, M. H.: Surf. Coat. Technol., *137*, 2001, p. 249.
[21] WILLIAMSON, D. L.—OZTURK, O.—WEI, R.—WILBUR, P. J.: Surf. Coat. Technol., *65*, 1994, p. 15.
[22] SINGH, V.—MARCHEV, K.—COOPER, C. V.—MELETIS, E. I.: Surf. Coat. Technol., *160*, 2002, p. 249.
[23] NOSEI, L.—AVALOS, M.—GOMEZ, B. J.—NACHEZ, L.—FEUGEAS, J.: Thin Solid Films, *468*, 2004, p. 134.
[24] BABA, H.—KODAMA, T.—KATADA Y.: Corros Sci., *44*, 2002, p. 2393.
[25] JARGELIUS-PETTERSSON, R. F. A.: Corros Sci., *41*, 1999, p. 1639.